

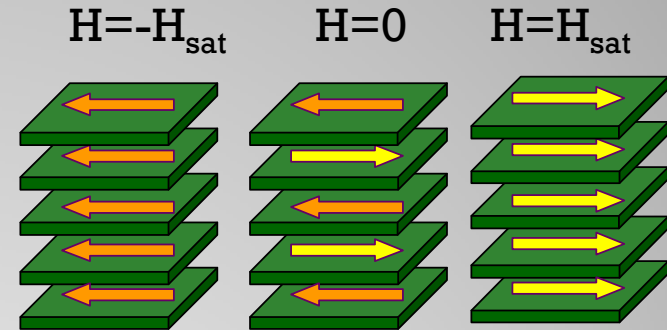
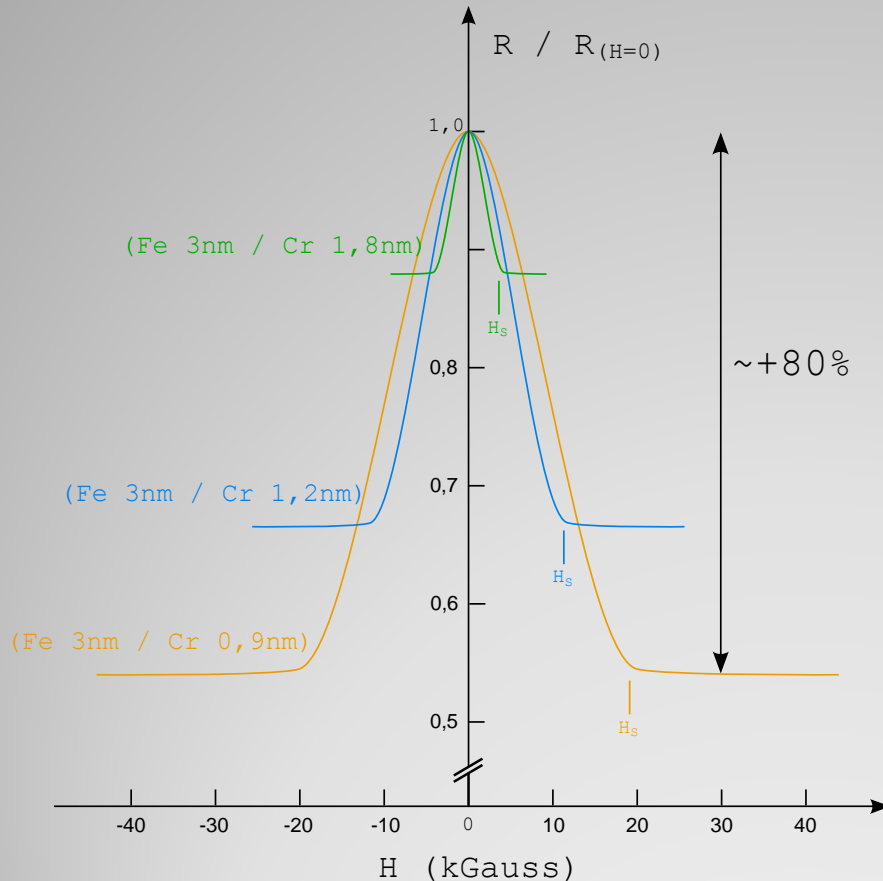
Spin as itinerant carrier of information

A. Vedyayev, N. Ryzhanova, N. Strelkov (*MSU*)
M. Chshiev, B. Dieny (*Spintec, France*)

- Giant magnetoresistance (GMR) and tunnel magnetoresistance (TMR) as fundamental spintronics
- Current in plane (CIP) and current perpendicular to plane (CPP) GMR
- Mechanisms of GMR and TMR
- Spin torque. Applications of GMR and TMR
 - Magnetic reading heads
 - Magnetic random access memory (MRAM)
 - Radio frequency oscillations RfO
- Spin Hall Effect (SHE) (Origin and possible applications)
- Conclusions

Scope

Birth of spin electronics : Giant MagnetoResistance discovery (1988)



$$GMR = \frac{R_{AP} - R_P}{R_P}$$

M. N. Baibich, J. M. Broto, A. Fert et al
Phys. Rev. Lett. **61**, 2472–2475 (1988)

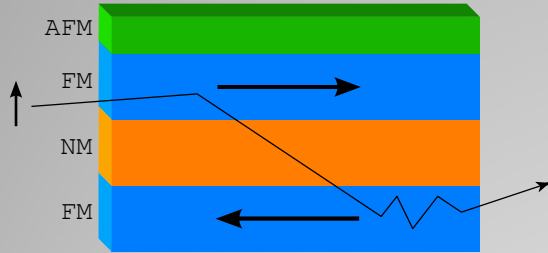
G. Binasch, P. Grünberg et al
Phys. Rev. B **39**, 4828–4830 (1989)

GMR due to spin-dependent scattering in the bulk or at the interfaces of the magnetic layers

Giant magnetoresistance (GMR)

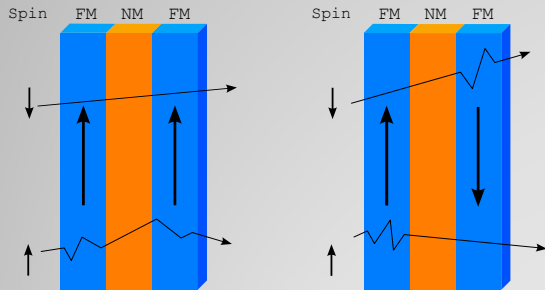
Giant MagnetoResistance in Spin-valve structure

Current In Plane (CIP) (Size effect)



$$\text{GMR} \sim e \frac{-t_{\text{NM}}}{l_{\text{NM}}}$$

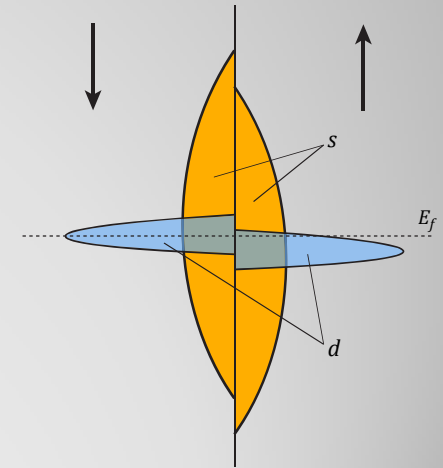
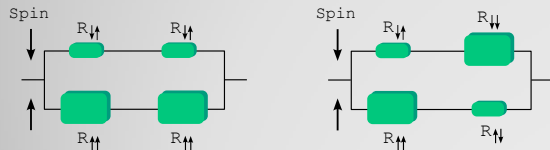
Current Perpendicular to Plane (CPP)



$$\rho \sim 1/\tau_{\text{sd}}^{\uparrow\downarrow} \sim \rho_{\text{d}}^{\uparrow\downarrow}$$

$$\Delta\rho \sim \beta^2 \rho_0 l_{\text{sf}}$$

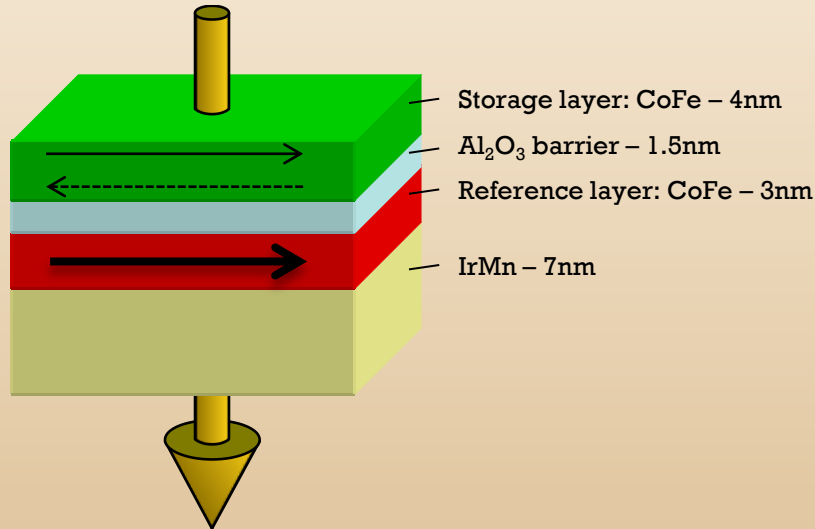
$$\text{GMR} = \frac{(\rho^{\uparrow} - \rho^{\downarrow})^2}{2\rho^{\uparrow}\rho^{\downarrow}}$$



Giant magnetoresistance (GMR)

Magnetic Tunnel Junctions and Tunnel MagnetoResistance

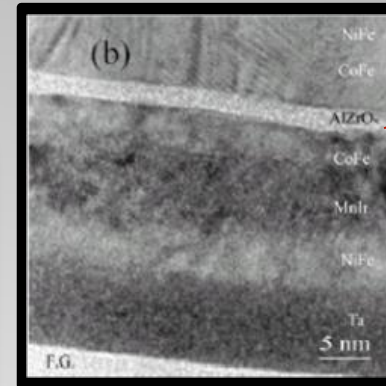
Structure of a magnetic tunnel junction



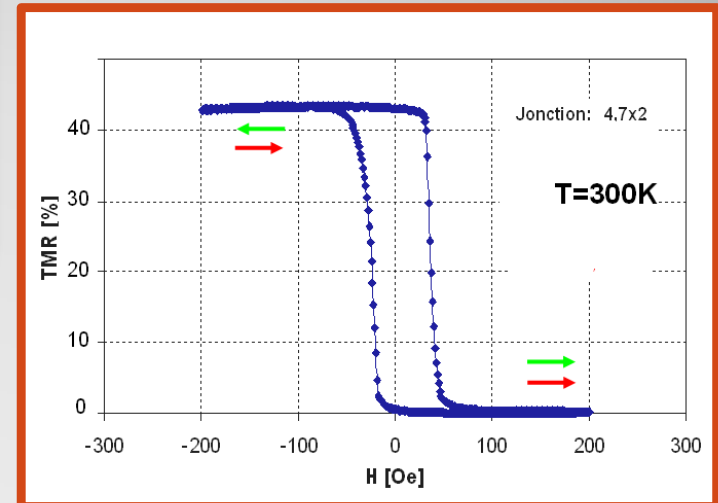
Acts as a couple polarizer/analyzer with the spin of the electrons.

M. Julliere, Phys. Lett. A **54** (1975)

J. S. Moodera et al, Phys. Rev. Lett. **74** (1995)

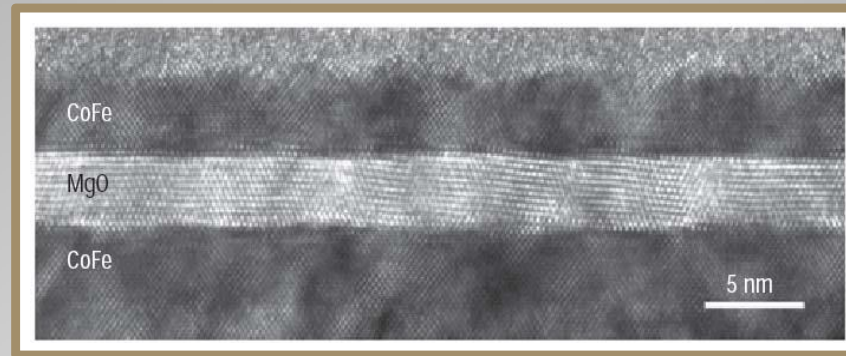


Al(Zr)O_x



Tunnel magnetoresistance (TMR)

Giant Tunnel MagnetoResistance of MgO tunnel barriers



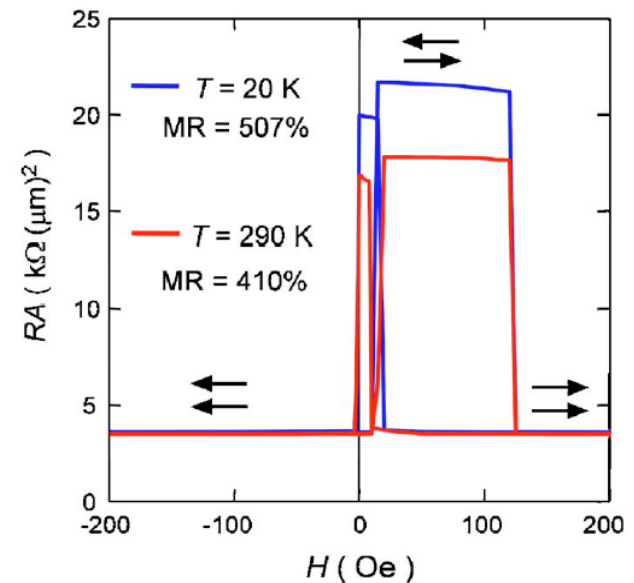
Very well textured MgO barriers grown by sputtering or MBE on bcc CoFe or Fe magnetic electrodes, or on amorphous CoFeB electrodes followed by annealing to recrystallize the electrode.

S.S.P.Parkin et al, Nature Mat. (2004), nmat 1256

S.Yuasa et al, Nature Mat. (2004), nmat 1257

S.Yuasa et al, Appl. Phys. Lett. **89** (2006)

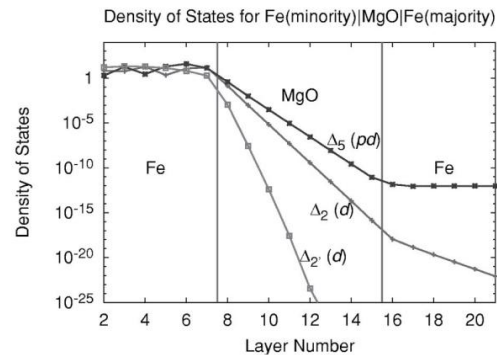
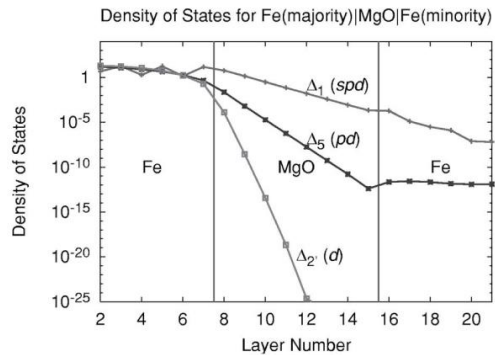
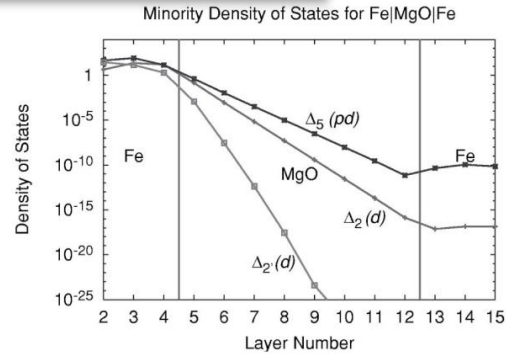
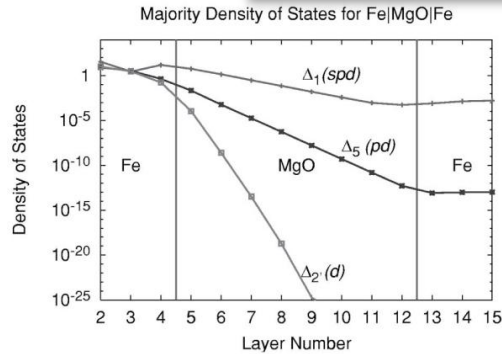
Au cap 50 nm
Ir-Mn 10 nm
Fe(001) 10 nm
Co(001) 0.57 nm
MgO(001) 2.2 nm
Co(001) 0.57 nm
Fe(001) 100 nm
MgO(001) 20 nm
MgO(001) sub.



Tunnel magnetoresistance (TMR)

Spin torque in Magnetic Tunnel Junction (Ballistic mode)

Tunneling Density Of States



Conf



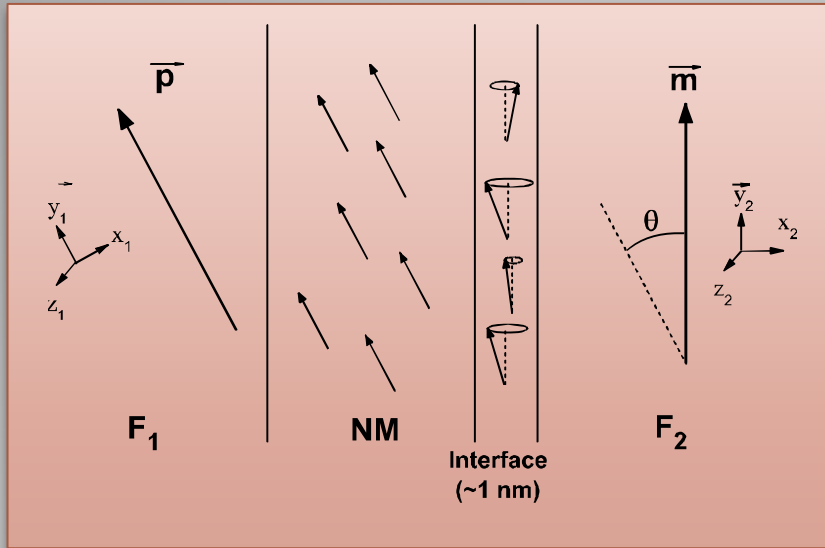
Spin



W. H. Butler *et al*, PHYSICAL REVIEW B, **63**, 054416

Spin Torque

Spin torque in magnetic metallic multilayers (Diffusive mode)



Schematics of the mechanism of spin transfer torque in a metallic trilayer. Polarized electrons flowing from left to right precess around the right layer magnetization with different frequencies due to their different incident angles at the interface. This results in ballistic interference yielding an oscillation and damping of spin torque near the interface (typically 1 nm)

Charge current

$$j_n^e = \frac{E_x}{\rho_n} - D_{0n} \frac{\partial n_n^0}{\partial x} - D_{0n} \beta' \left(M_n^x \frac{\partial m_n^x}{\partial x} + M_n^y \frac{\partial m_n^y}{\partial x} + M_n^z \frac{\partial m_n^z}{\partial x} \right)$$

Spin current

$$\vec{j}_n^m = \frac{\beta_n E_x \vec{M}_n}{\rho_n} - D_{0n} \beta' \vec{M}_n \frac{\partial n_n^0}{\partial x} - D_{0n} \frac{\partial \vec{m}_n}{\partial x}$$

$$D_n^{\uparrow(\downarrow)} = D_{0n} (1 \pm \beta'_n)$$

$$1/\rho_n^{\uparrow(\downarrow)} = (1 \pm \beta_n) / 2\rho_n$$

T. Valet and A. Fert *Phys. Rev. B* **48** (1993)

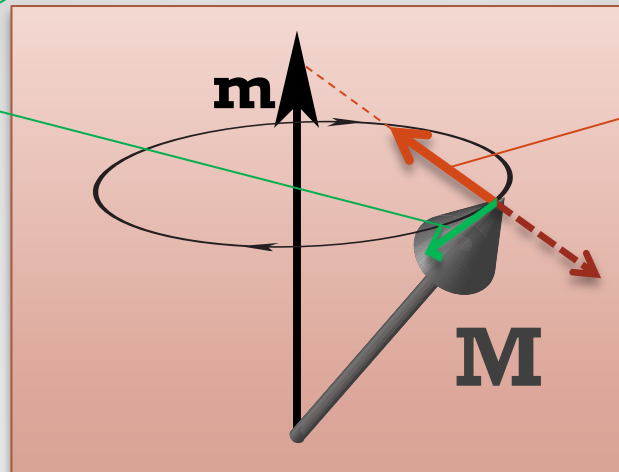
Spin Torque

Spin torque and LLG equation

$$\frac{\partial \vec{M}}{\partial t} = -\gamma \left[\vec{M} \times \vec{H}_{\text{eff}} \right] + \frac{\alpha}{M_s} \left[\vec{M} \times \frac{\partial M}{\partial t} \right] + \gamma \vec{T}$$

$$\vec{T} = \vec{T}_{\perp} + \vec{T}_{\parallel} = b \left[\vec{M} \times \vec{m} \right] + \frac{a}{M_s} \left[\vec{M} \times \left[\vec{M} \times \vec{m} \right] \right]$$

Torque perpendicular
to plane (M, m)



Torque in plane (M, m)

Spin Torque

Spin torque in magnetic metallic multilayers (Diffusive mode)

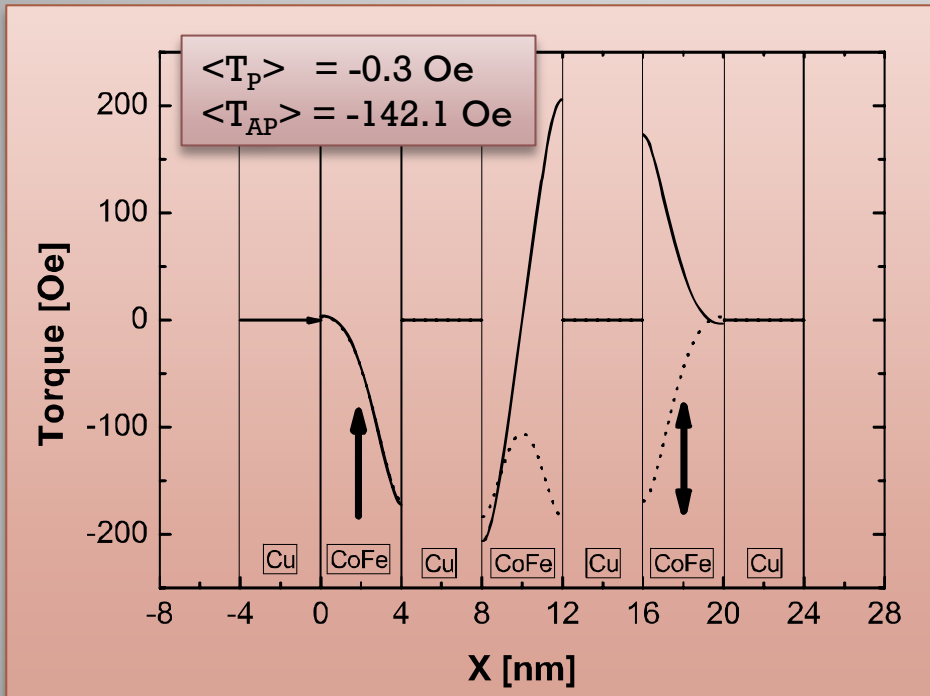
Conditions for non-divergent current components

$$\frac{\partial j_n^e}{\partial x} = 0$$

$$\frac{\partial \vec{j}_n^m}{\partial x} + \frac{J}{\hbar} [\vec{m}_n \times \vec{M}_n] + \frac{\vec{m}_n}{\tau_{nsf}} = 0$$

$$\lambda_{sf}^2 = D\tau$$

$$\lambda_J^2 = iD \frac{\hbar}{J}$$



Material parameters used in the simulations. The interfacial resistance (r) and interfacial spin asymmetry (γ) are introduced for modeling *CoFe/Cu* interfaces:

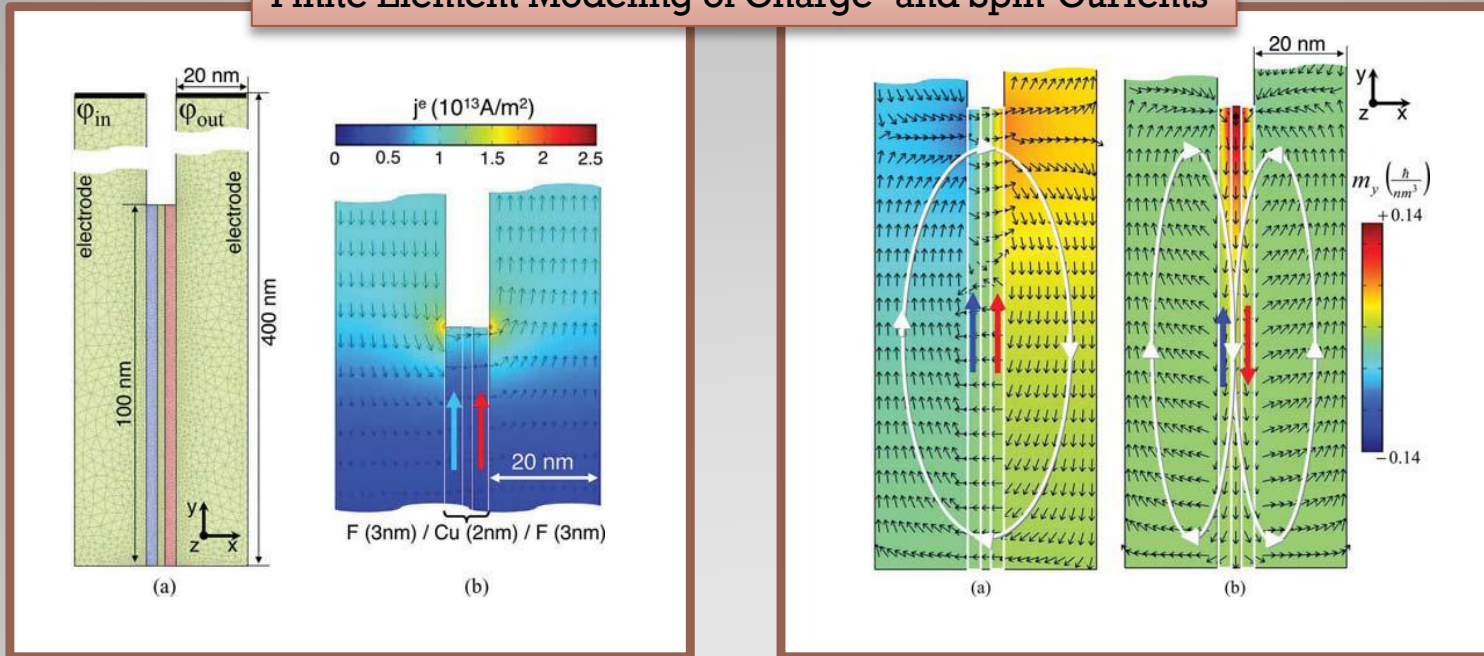
	ρ ($\mu\Omega \text{ cm}$)	β	δ	r ($\text{m}\Omega \mu\text{m}^2$)	γ	λ_{sf} (nm)	λ_J (nm)
CoFe	19	0.55	0.75	40	0.7	15	1
Cu	5	0	0	40	0.7	100	

Dependence of the spin torque on the coordinate X , perpendicular to the planes of the layers for the values of parameters depicted in table. Spin torque is given for parallel (solid line) and antiparallel (dotted line) configurations of the pinned layers. T is the spin torque in the free layer, averaged over its thickness.

Spin Torque

Spin torque in magnetic metallic multilayers (Diffusive mode)

Finite Element Modeling of Charge- and Spin-Currents



Scheme of studied magnetoresistive nanopillar sandwiched between two extended electrodes. The nanopillar composition is a model sandwich of the form F3 nm/Cu2 nm/F3 nm in which F is a ferromagnetic metal.

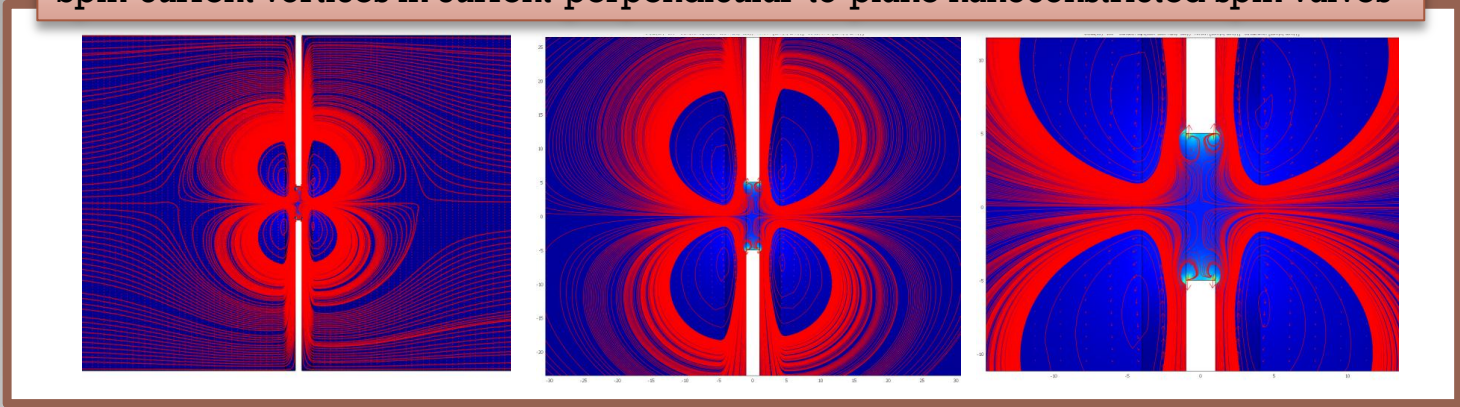
Zoom around the magnetoresistive pillar showing the y-component of spin current flow throughout the system in (a) parallel magnetic configuration, (b) antiparallel configuration. The normalized arrows indicate the spin current flow.

N. Strelkov, A. Vedyayev *et al*, IEEE MAGNETICS LETTERS, **Volume 1** (2010)

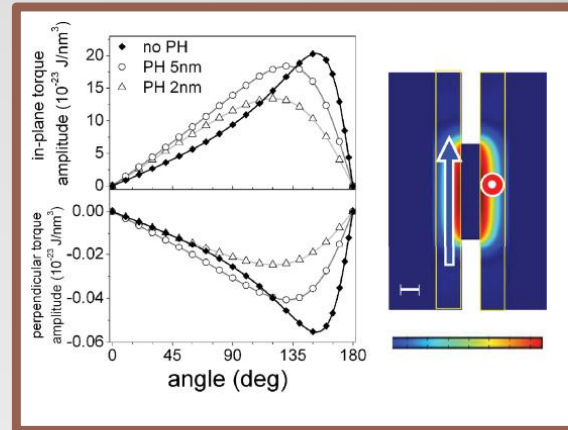
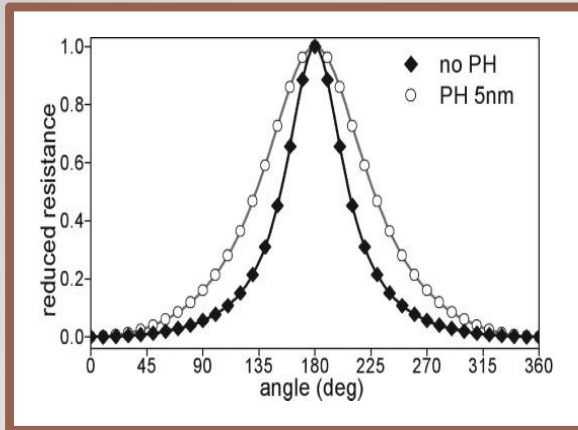
Spin Torque

Spin torque in magnetic metallic multilayers (Diffusive mode)

Spin-current vortices in current-perpendicular-to-plane nanoconstricted spin valves



Angular variation of the CPP-reduced resistance for the constriction of the 5-nm diameter and continuous spacer. The dots are the calculated values, and the lines are fits according to Slonczewski's expression.



In-plane and (b) perpendicular components of averaged spin-transfer torque over the whole volume of the "free" (right) magnetic layer as a function of the angle between the magnetizations.

N. Strelkov, A. Vedyayev *et al*, PHYSICAL REVIEW B **84**, 024416 (2011)

Spin Torque

Spin torque in Magnetic Tunnel Junction (Ballistic mode)

Spin torque definition

$$m_x + im_y = \langle \sigma^+ \rangle = \left\langle \left(\Psi^\uparrow \quad \Psi^\downarrow \right) \begin{pmatrix} 0 & 2 \\ 0 & 0 \end{pmatrix} \begin{pmatrix} \Psi^{*\uparrow} \\ \Psi^{*\downarrow} \end{pmatrix} \right\rangle = 2 \langle \Psi^\uparrow \Psi^{*\downarrow} \rangle$$

m_x – Interlayer Exchange Coupling (**IEC**)

m_y – Spin Transfer Torque (**STT**)

Ψ – Hartree-Fock spinor

$\langle \sigma^+ \rangle = \langle \sigma^x + i\sigma^y \rangle$

Keldysh Green function

$$G_{\uparrow\downarrow}^{-+}(\mathbf{r}, \mathbf{r}') = \int d\epsilon \left\{ f_L [\Psi_L^{\downarrow(\uparrow)*}(\mathbf{r}') \Psi_L^{\uparrow(\uparrow)}(\mathbf{r}) + \Psi_L^{\downarrow(\downarrow)*}(\mathbf{r}') \Psi_L^{\uparrow(\downarrow)}(\mathbf{r})] \right. \\ \left. + f_R [\Psi_R^{\downarrow(\uparrow)*}(\mathbf{r}') \Psi_R^{\uparrow(\uparrow)}(\mathbf{r}) + \Psi_R^{\downarrow(\downarrow)*}(\mathbf{r}') \Psi_R^{\uparrow(\downarrow)}(\mathbf{r})] \right\}$$

Schrödinger equation

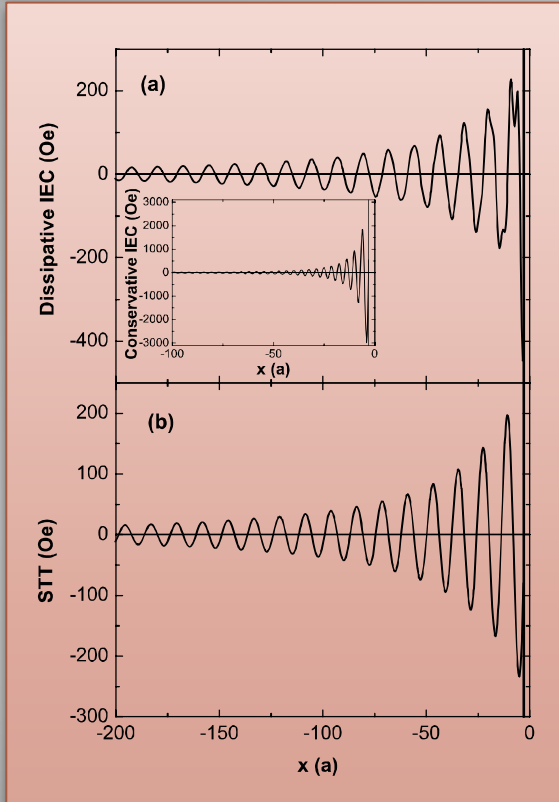
$$H \Psi = \left(\frac{p^2}{2m} - U - J_{sd}(\vec{\sigma} \cdot \vec{S}_d) \right) \begin{pmatrix} \Psi^\uparrow \\ \Psi^\downarrow \end{pmatrix} = E \begin{pmatrix} \Psi^\uparrow \\ \Psi^\downarrow \end{pmatrix}$$

S_d – local magnetization of d-electrons

Spin Torque

Spin torque in Magnetic Tunnel Junction (Ballistic mode)

$$m_x + im_y = \frac{J_{sd}}{\mu_B} \langle \sigma^+ \rangle = \frac{J_{sd}}{\mu_B} \frac{a_0^3}{(2\pi)^2} \int \int G_{\uparrow\downarrow}^{-+}(x, x, \epsilon) \kappa \, d\mathbf{k} \, d\epsilon$$



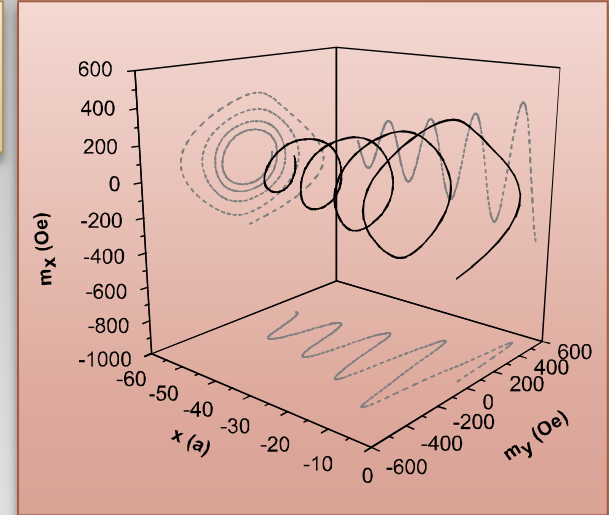
Parameters

$$\begin{aligned} \epsilon \downarrow &= -1.37 \text{ eV} \\ V_b &= 0.1 \text{ V} \end{aligned}$$

A. Manchon *et al*
J. Phys.: Cond. Mat. **19** (2007) 165212

A. Manchon *et al*
J. Phys.: Cond. Mat. **20** (2008) 145208

Total spin density as a function of the location in the left electrode. (a) Current-induced interlayer exchange coupling; inset, interlayer exchange coupling at zero bias voltage. (b) Spin transfer torque.



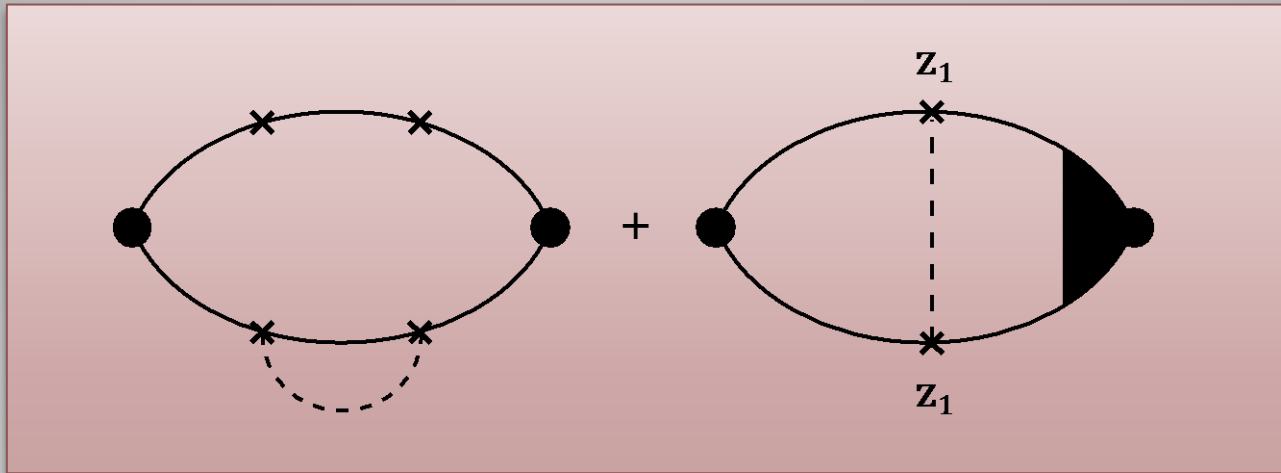
Transfer spin density (black line) as a function of the distance in the left ferromagnetic electrode in a usual ferromagnetic regime.

Torque

$$\vec{T} = -\gamma \left[\vec{S}_d \times \vec{m} \right]$$

Spin Torque

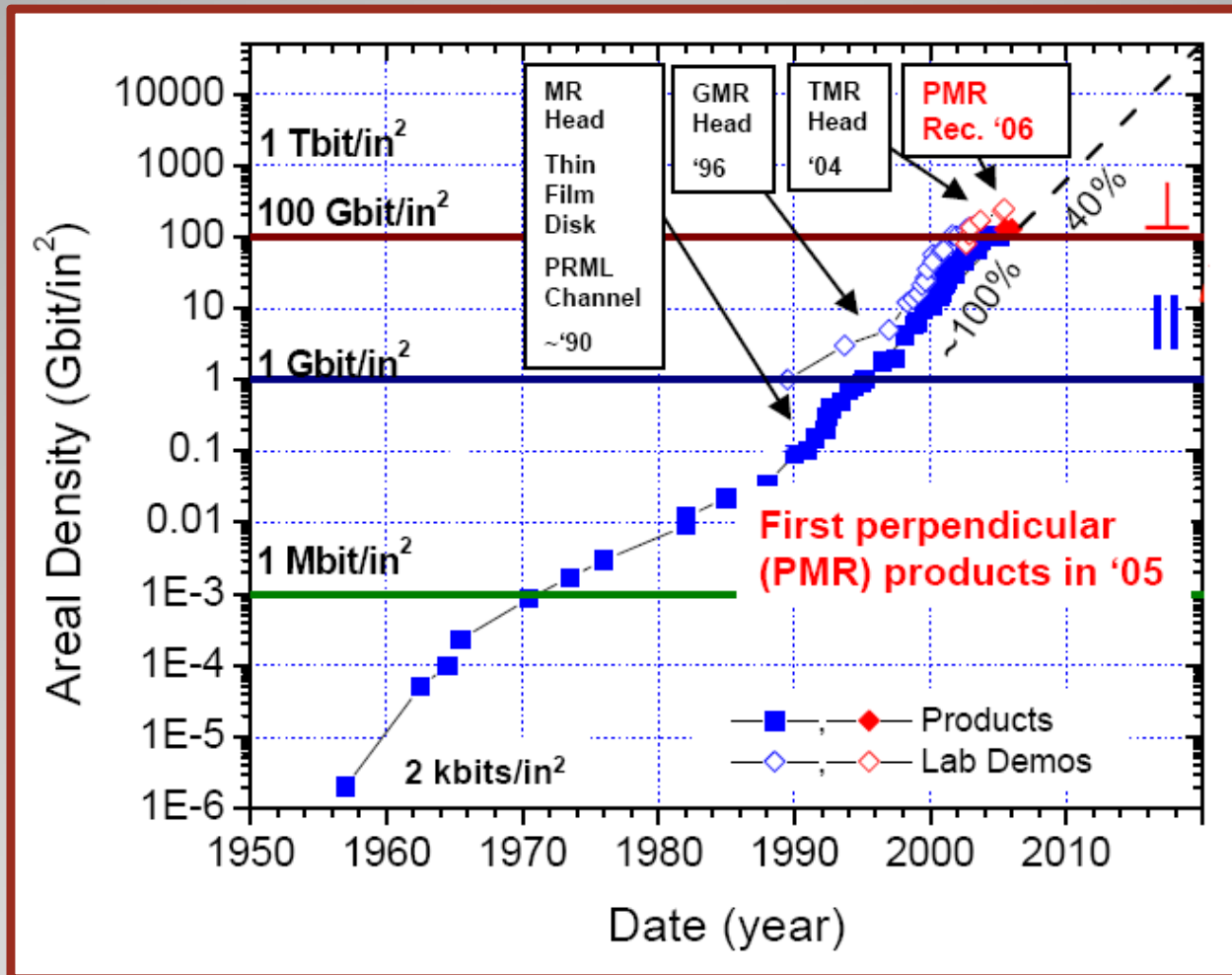
Problem



$$G(z, z') \neq G(z - z')$$

Spin Torque

Dramatic increase in areal storage density over the past 50 years



Applications

Benefit of GMR in magnetic recording



**GMR spin-valve heads
from 1998 to 2004**

Applications

**Magnetic Tunnel Junctions (MTJ):
a reliable path for CMOS/magnetic integration**

Resistance of MTJ compatible with resistance of passing FET (few $k\Omega$)

MTJ can be deposited in magnetic back end process

No CMOS contamination

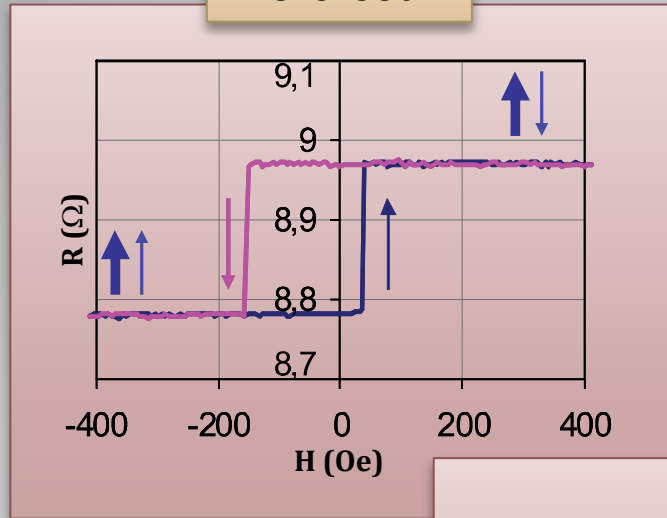
MTJ used as variable resistance controlled by field or current/voltage (Spin-transfer)

Commercial CMOS/MTJ products available from EVERSPIN since 2006 (4Mbit MRAM) implemented in Airbus flight controller

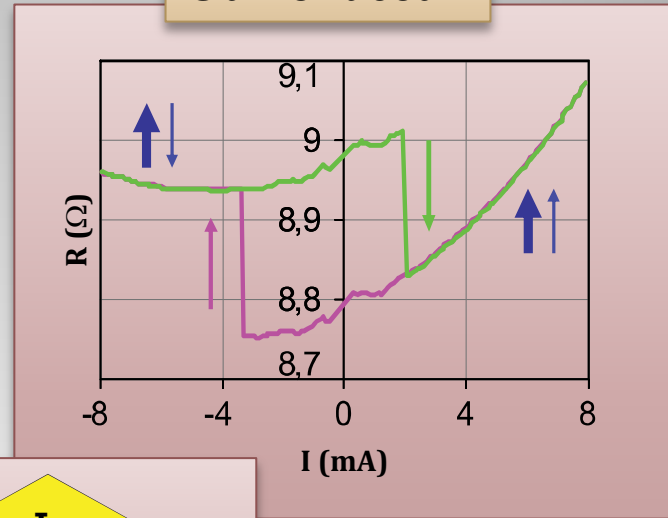
Applications

Magnetization switching induced by a polarized current

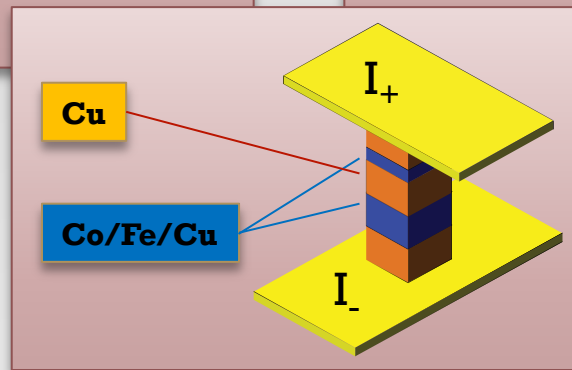
Field scan



Current scan



Can be used as a **new write scheme in MRAM** or to generate steady state oscillations leading to **RF oscillators**



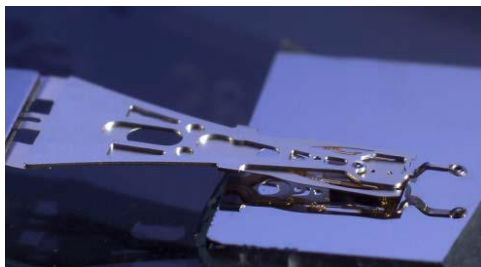
By spin transfer, a spin-polarized current can be used to manipulate the magnetization of magnetic nanostructures instead of by magnetic field.

J. C. Katine et al
Phys.Rev. Lett. **84**, 3149 (2000)

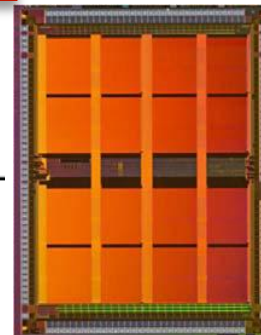
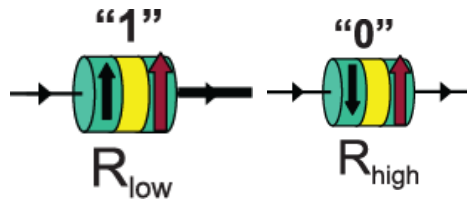
Applications

Spintronic components

Magnetic field sensors

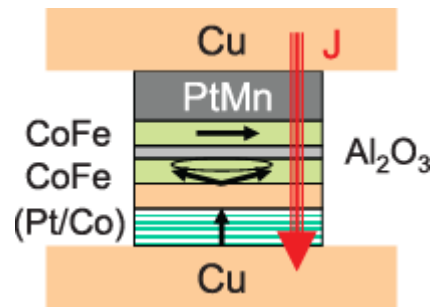


Memories



$$KV > 50 \div 100 k_B T$$

RF components

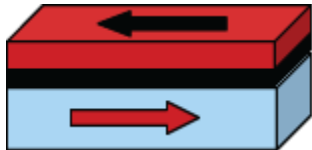


Applications

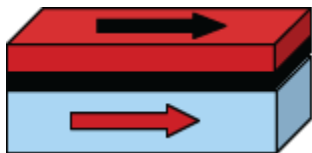
Field induced magnetic switching (FIMS) MRAM

Bit states

“1”

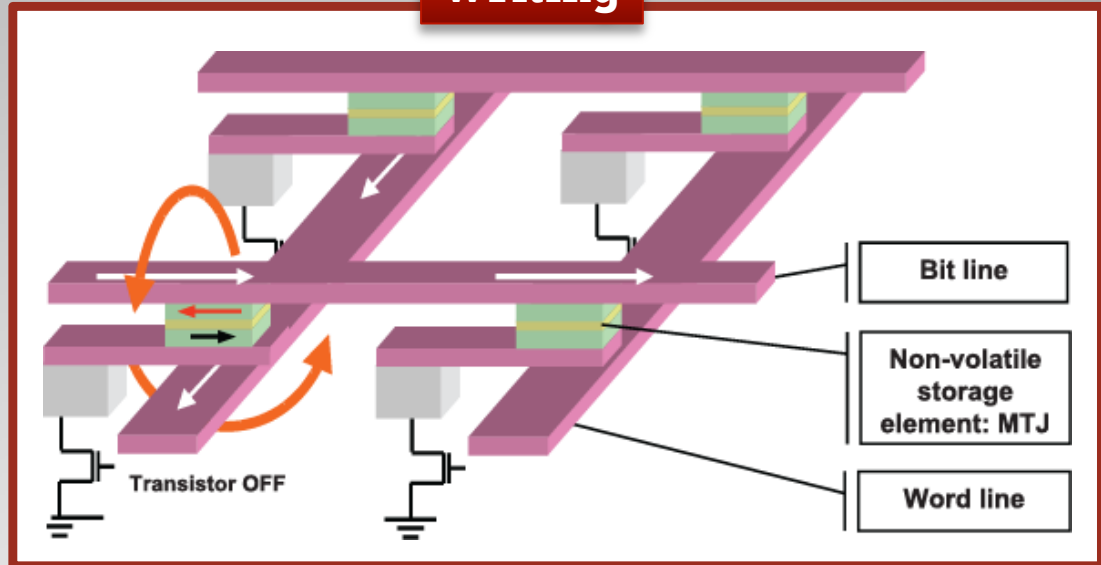


“0”

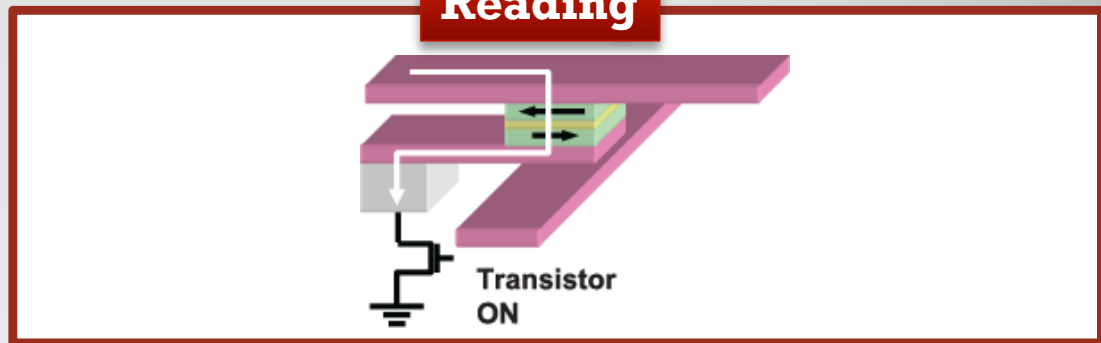


Store data by the direction (parallel or antiparallel) of magnetic layers in MTJ

Writing

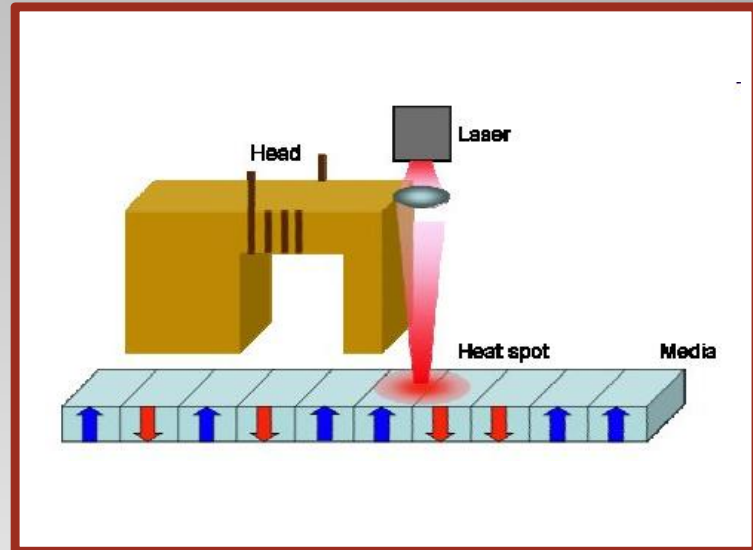
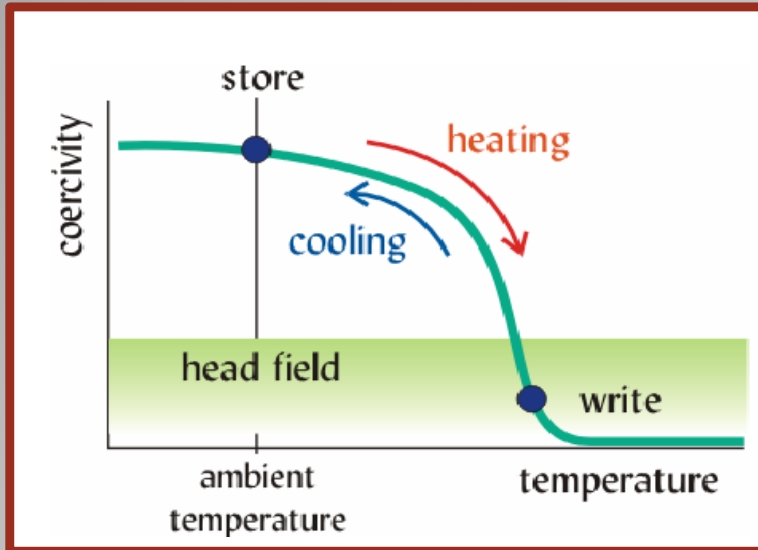


Reading



Applications

Thermally Assisted switching (TAS)



Use temperature-dependence of switching ability:

Write at elevated temperature

Store / read at room temperature

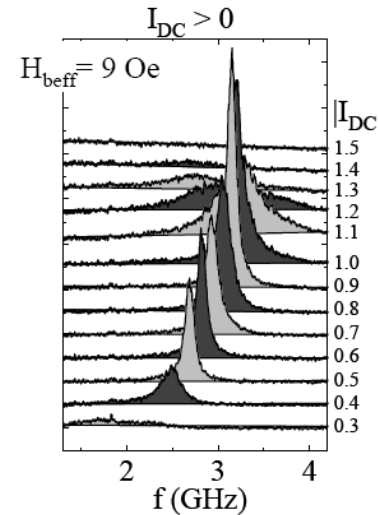
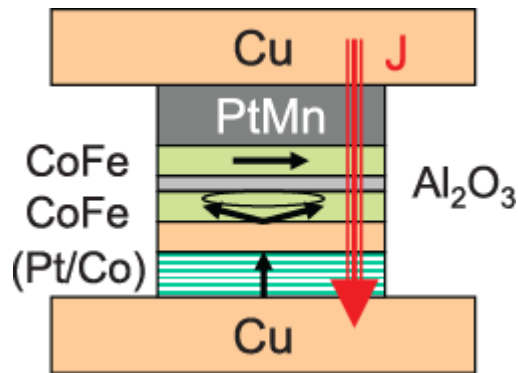
In MTJ for MRAM, heating produced by Joule dissipation around the tunnel barrier

Write temperature $\sim 250^{\circ}\text{C}$

Applications

RF components based on spin transfer

RF oscillator with perpendicular to plane polarizer



D. Houssameddine et al
Nature Materials **6**,
447 - 453 (2007)

K. J. Lee et al
Appl. Phys. Lett. **86**,
022505 (2005)

Injection of electrons with out-of-plane spins

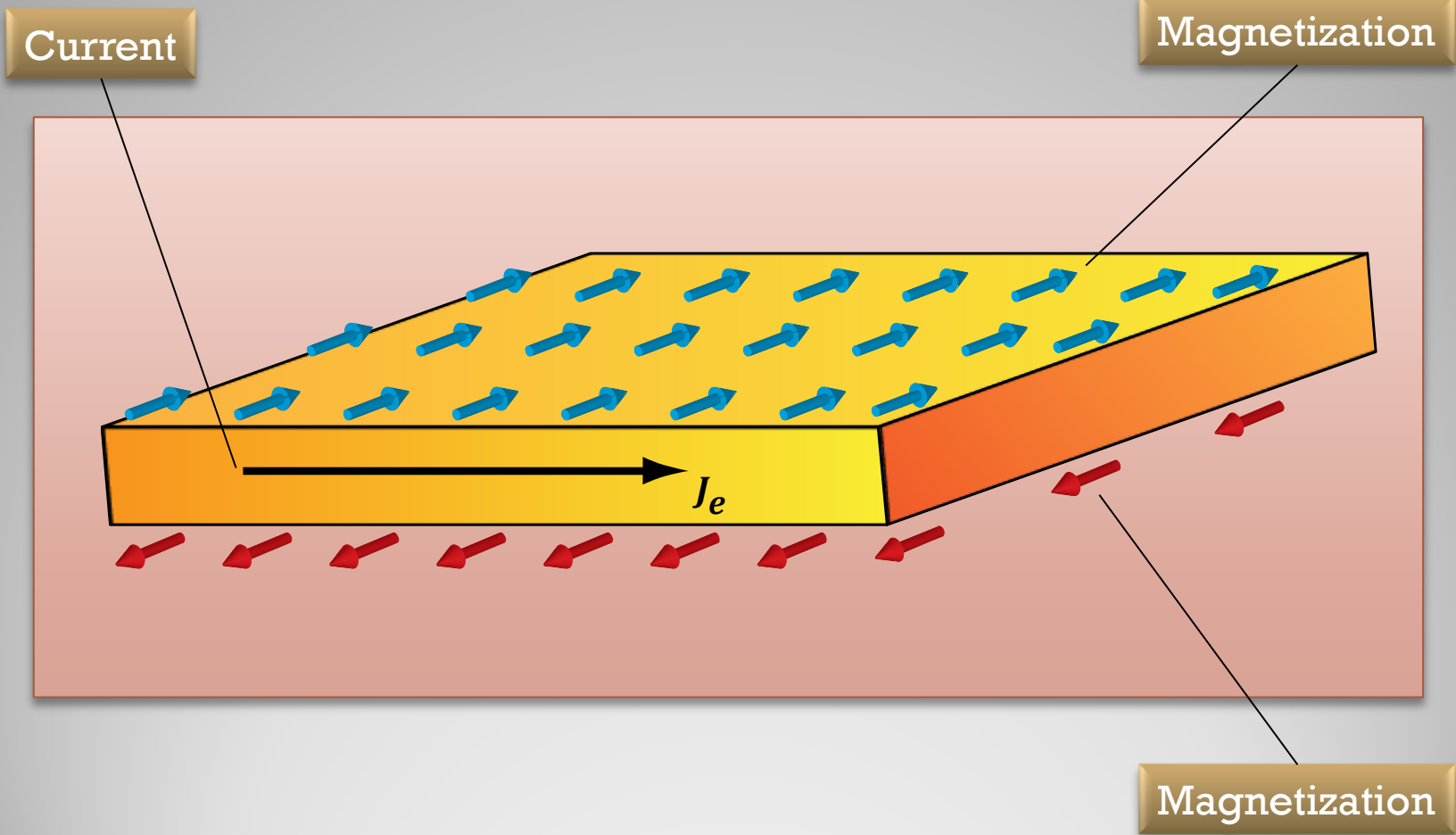
Steady precession of the magnetization of the soft layer adjacent to the tunnel barrier.

Precession (2GHz-40GHz) + Tunnel MR \Rightarrow RF voltage

Interesting for frequency tunable RF oscillators \Rightarrow Radio opportunism

Applications

Spin Hall effect



Spin Hall

Spin Hall (diffusion model)

Charge current

$$\vec{j}_e = -\sigma_0 \vec{\nabla} \varphi - \beta \frac{\sigma_0}{e\nu} \vec{\nabla} (\vec{U}_M, \vec{m}) + a_0^3 \sigma_{\text{SH}} [\vec{m} \times \vec{\nabla} \varphi]$$

Spin current

$$\vec{j}_m^{(i)} = -\beta \sigma_0 \vec{\nabla} \varphi U_M^{(i)} - \frac{\sigma_0}{e\nu} \vec{\nabla} m^{(i)} - \sigma_{\text{SH}} U_m^{(i)} [\vec{U}_m \times \vec{\nabla} \varphi]$$

System of equations

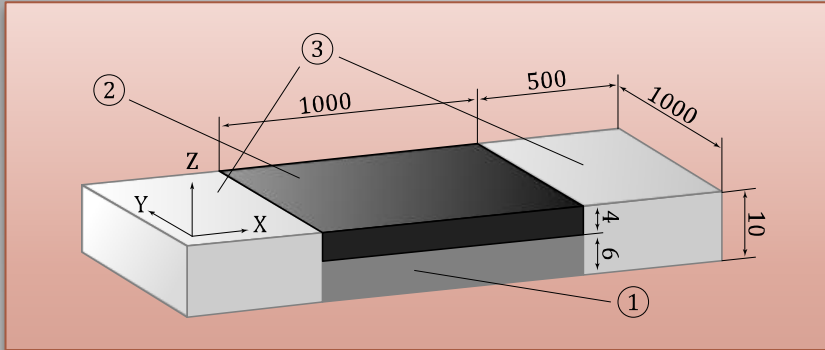
$$\begin{cases} \operatorname{div} \vec{j}_e = 0 \\ \operatorname{div} \vec{j}_m^{(i)} = -\frac{\sigma_0}{e^2 \nu l_J^2} [\vec{m} \times \vec{U}_M]^{(i)} - \frac{\sigma_0}{e^2 \nu l_{\text{sf}}^2} m^{(i)} \end{cases}$$

$$\vec{U}_M = \frac{\vec{M}}{M_s}$$

$$\vec{U}_m = \frac{\vec{m}}{|\vec{m}|}$$

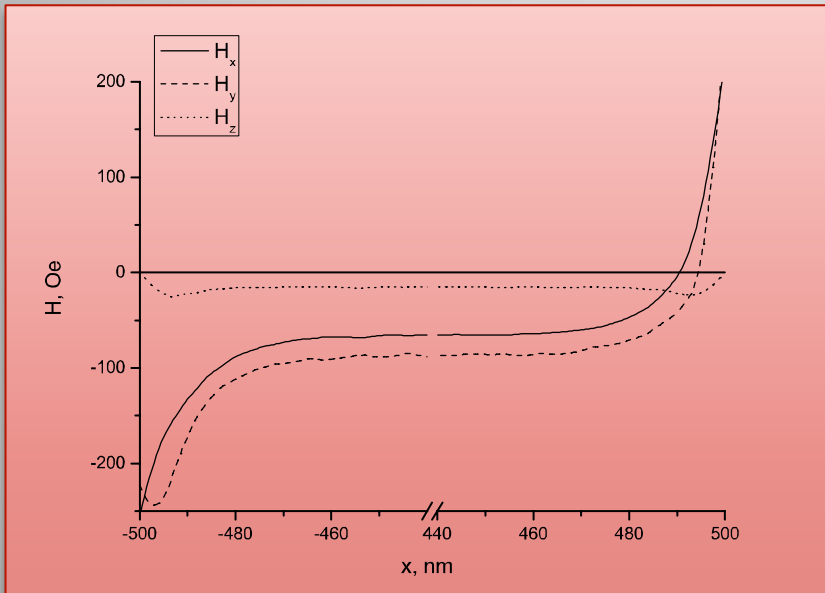
Spin Hall

Spin Hall in Pt/Py bylayer of size 1000 nm



Schematic of Pt/Py bylayer.

Sizes are in “nm”. 1 – Pt layer, 2 – Py layer, 3 – Cu electrodes. Current is along x axe. Magnetisation of Py is in xy plane at $\pi/4$ angle to x axe.



Effective fields induced by Pt SHE in Py near the interface.

Adopted values of the parameters:

$$\sigma^{\text{Pt}} = 0.005 (\Omega \text{ nm})^{-1},$$

$$L_{\text{sf}}^{\text{Pt}} = 10 \text{ nm},$$

$$\sigma_{\text{SH}}^{\text{Pt}} = 0.1 \sigma^{\text{Pt}},$$

$$\sigma^{\text{Py}} = 0.0022 (\Omega \text{ nm})^{-1},$$

$$l_{\text{sf}}^{\text{Py}} = 6 \text{ nm},$$

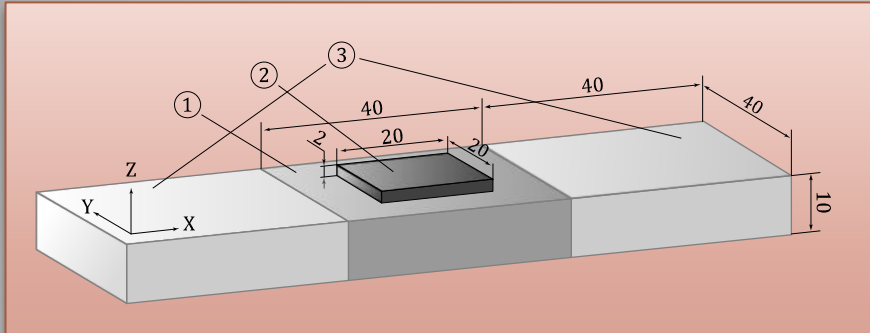
$$\beta = 0.7,$$

$$L_{\text{J}} = 1 \text{ nm},$$

$$\text{current density } j = 10^7 \text{ A/cm}^2$$

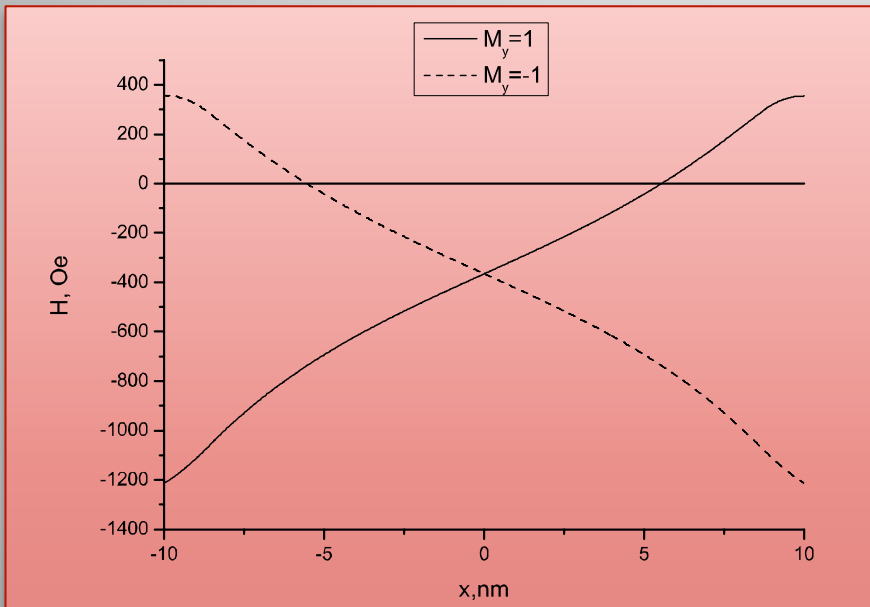
Spin Hall

Spin Hall in Pt/Py bylayer of size 20 nm



Schematic of Pt/Py bylayer.

Sizes are in “nm”. 1 – Pt layer, 2 – Py layer, 3 – Cu electrodes. Current is along x axe. Magnetisation of Py is in xy plane at $\pi/4$ angle to x axe or along z axe.



Effective fields in Co/Pt structure for the direction of magnetization parallel and antiparallel to y axe.

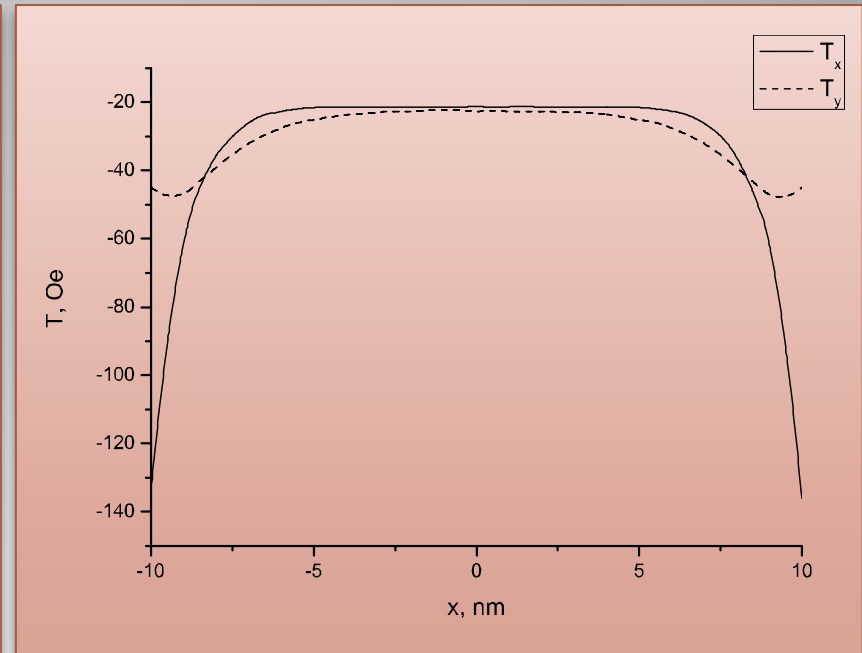
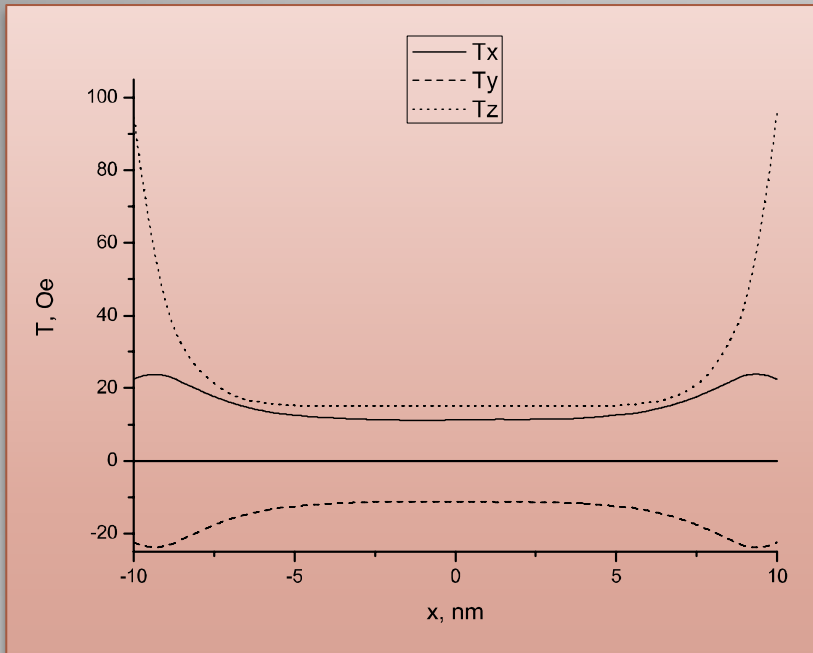
Only H_y component survive. Values of the parameters:

$$\sigma^{\text{Co}} = 0.005 (\Omega \text{ nm})^{-1},$$

$$L_{\text{sf}}^{\text{Co}} = 10 \text{ nm}$$

Spin Hall

Spin Hall in Pt/Py bilayer of size 20 nm



Effective torques for the case of $U_M = (\cos \pi/4; \sin \pi/4; 0)$ near the interface.

Averaged values over volume of Co are:

$$\langle T_x \rangle = 15 \text{ Oe}, \langle T_y \rangle = -15 \text{ Oe},$$

$$\langle T_z \rangle = 3 \text{ Oe}$$

Effective torques near the interface in case of $M \parallel Oz$. Averaged values over volume of Co are:

$$\langle T_x \rangle = -4 \text{ Oe}, \langle T_y \rangle = -30 \text{ Oe}$$

Spin Hall

1. The mechanisms responsible for GMR, TMR and STT are well established
2. The mechanisms limiting the value of GMR and TMR, especially for half-metallic ferromagnets (CrO_2 , Heusler alloys NiMgSb) has to be clarified
3. The theory describing the diffusive and ballistic spin spin transport on the same footing is still absent
4. Hybrid ferromagnetic/SHE structures may be effective tools for manipulation with magnetic configuration
5. MRAM and other magnetic devices may compete with CMOS in microelectronics

Conclusions

**Thank you
for attention**